Intercomparison of Calorimetry, Raman Spectroscopy, and Second Harmonic Generation Applied to Solid−Solid Phase Transitions

L. Smilowitz,* B. F. Henson, and J. J. Romero

Chemistry Division, Los Alamos National Laboratory, Los Alamos, New Mexico 87545

Received: March 9, 2009; Revised Manuscript Received: June 17, 2009

This paper compares several different observables for use in measuring the kinetics of solid−solid phase transitions. Relative advantages and disadvantages for each technique are described, and a direct comparison of results is made for the beta to delta polymorphic phase transition of the energetic nitramine, octahydro-1,3,5,7-tetranitro-1,3,5,7-tetrazocine.

Introduction

The study of solid−solid phase transformations is hindered by the difficulty of finding a volumetric probe to use as a progress variable. Solids are typically optically opaque and heterogeneous. Over the past several years, second harmonic generation (SHG) has been used as a kinetic probe for a solid−solid phase transition in which the initial and final phases have different symmetries. Bulk generation of SHG is allowed by symmetry only in noncentrosymmetric crystallographic space groups. For the organic energetic nitramine octahydro-1,3,5,7-tetranitro-1,3,5,7-tetrazocine (HMX), the initial beta phase is centrosymmetric (space group $P2_1/c$) and the final delta phase is noncentrosymmetric (space group $P6_122$) making SHG an extremely sensitive, essentially zero background probe of the phase change progress. We have used SHG as a tool to follow the progress of the transformation from beta to delta phase during the solid−solid transformation.[1,2] However, kinetic models of the transformation derived using different observables from several other groups have differed, showing later onset for the phase change and faster progression to completion.[3−5] In this work, we have intercompared several techniques to understand these differences. The three techniques discussed are second harmonic generation, Raman spectroscopy, and differential scanning calorimetry (DSC). The progress of the beta to delta phase transition in HMX observed with each of these different probes will be discussed and advantages and disadvantages of each technique described.

Experimental Techniques

The three experimental techniques compared in this paper are second harmonic generation, Raman spectroscopy, and differential scanning calorimetry. SHG measurements are carried out using 1064 nm wavelength laser light as the probe and detecting the 532 nm light produced by the sample. Picosecond and nanosecond laser sources are used. The nonlinear nature of the response makes shorter pulses preferred due to the signal dependence on peak intensity. However, in order to couple measurements with calorimetry, fiber coupling is necessary leading to the use of nanosecond pulses due to the burn threshold of the fiber end at laser injection. Differential scanning calorimetry is performed using a commercial TG/DSC instrument from Netszch Instruments which has been modified to allow the incorporation of a fiber optic probe for simultaneous SHG/DSC/TG measurements as shown schematically in Figure 1. Raman spectroscopy is performed using a commercial fiber coupled instrument from Kaiser Optics using a 785 nm laser pump in order to reduce the effect of fluorescence. Simultaneous Raman and SHG measurements are performed both by measuring SHG in transmission and by beam splitting the 532 nm from the longer wavelength Raman stokes lines.

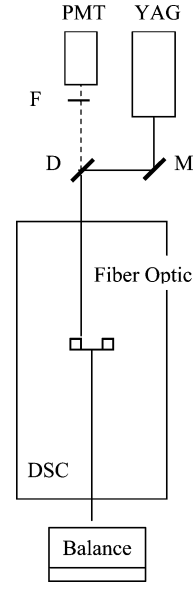

Figure 1. Experimental schematics DSC/SHG. M is a turning mirror, D a dichroic mirror reflecting 1064 nm and transmitting 532 nm, and F a filter to block scattered 1064 nm light and transmit only 532 nm SHG.

Samples used are both pure HMX crystals, and HMX in the PBX 9501 formulation which includes a binder consisting of Estane and the nitroplasticizer, BDNPA/F. The effect of the binder on phase transition kinetics has been discussed previously.[6]

Results

Figure 2 shows the onset of SHG for HMX crystals heated through the phase transition with different ramp rates. The peak SHG signal has been normalized to 1 in each case, and the time axes have been shifted for comparison. The SHG is seen to rise and then fall as the sample is heated past the phase transition

* Author to whom correspondence should be addressed. E-mail: smilo@lanl.gov. Phone: (505) 667-5207. Fax: (505) 667-0440.

10.1021/jp902111c CCC: $40.75
Published on Web 08/07/2009

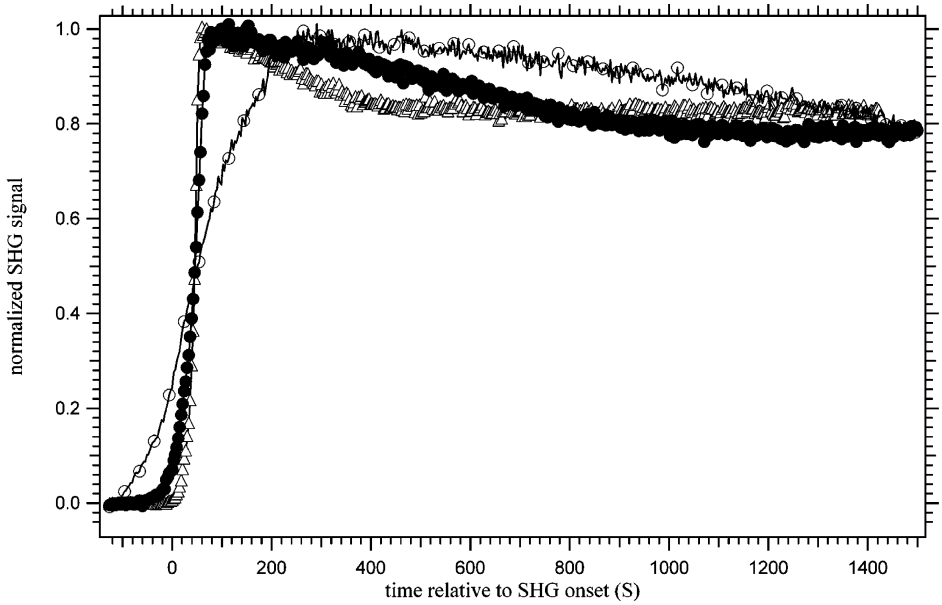

Figure 2. Ramp rate dependence of the onset of SHG. Open triangles, 10 °C/min; filled circles, 3 °C /min; open circles, 1 °C /min.

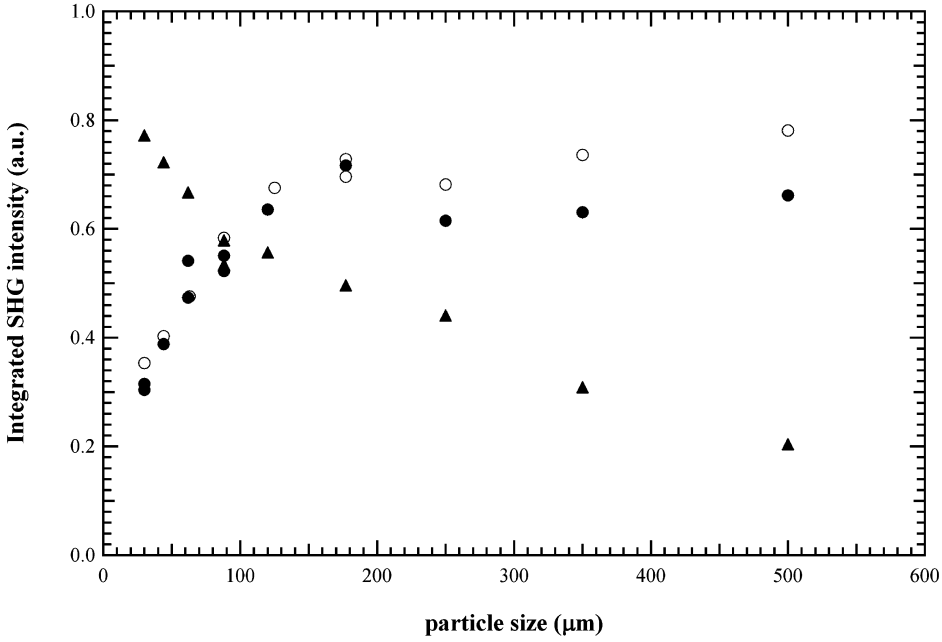

Figure 3. HMX phase matchability. Solid circles are HMX, open circles KDP, and solid triangles rhamnose.

temperature. The cause of the decrease is either a change in phase or a change in material state, such as a discoloration causing self-absorption of the second harmonic light. We have observed the phase directly in other Raman experiments to be described below and verified that the delta phase persists throughout these experiments. The subsequent decrease in intensity is therefore some function of the material state, not relevant to the conversion process under study here. The onset and slope of the SHG are both affected by rate in a way that is reproduced by the nucleation and growth model discussed previously.[2,7,8]

The use of SHG as a progress variable for formation of delta HMX is enabled by the change in crystallographic space group from centrosymmmetric to noncentrosymmetric upon transition from beta to delta phase. The intensity of the SHG signal in the delta phase is due in part to the phase matchability of the HMX delta crystals. Phase matching refers to the condition in a crystal where the wavelength dependent index of refraction allows for constructive interference between the fundamental and second harmonic generated on propagation through the crystal. This is a necessary condition for high efficiency generation of second harmonic light. Kurtz et al. developed a way to discern phase matchability based on the particle size dependence of SHG generation efficiency from powder samples.[9−11] The particle size dependence of SHG efficiency for HMX, potassium dihydrogen phosphate (KDP), and rhamnose is shown in Figure 3. All are organic crystals. KDP is a phase matchable crystal often used in lasers for harmonic generation. Rhamnose is a nonphase matchable sugar.[9] The two curves exhibited by the phase matchable KDP and nonphase matchable rhamnose are the classic curves first determined by Kurtz et al.[10] The particle size dependence exhibited by HMX follows that of KDP and is thus consistent with phase matchable behavior. The importance of this determination has to do with the dependence of SHG intensity on concentration (or fraction of the sample generating SHG). Phase matchability, and

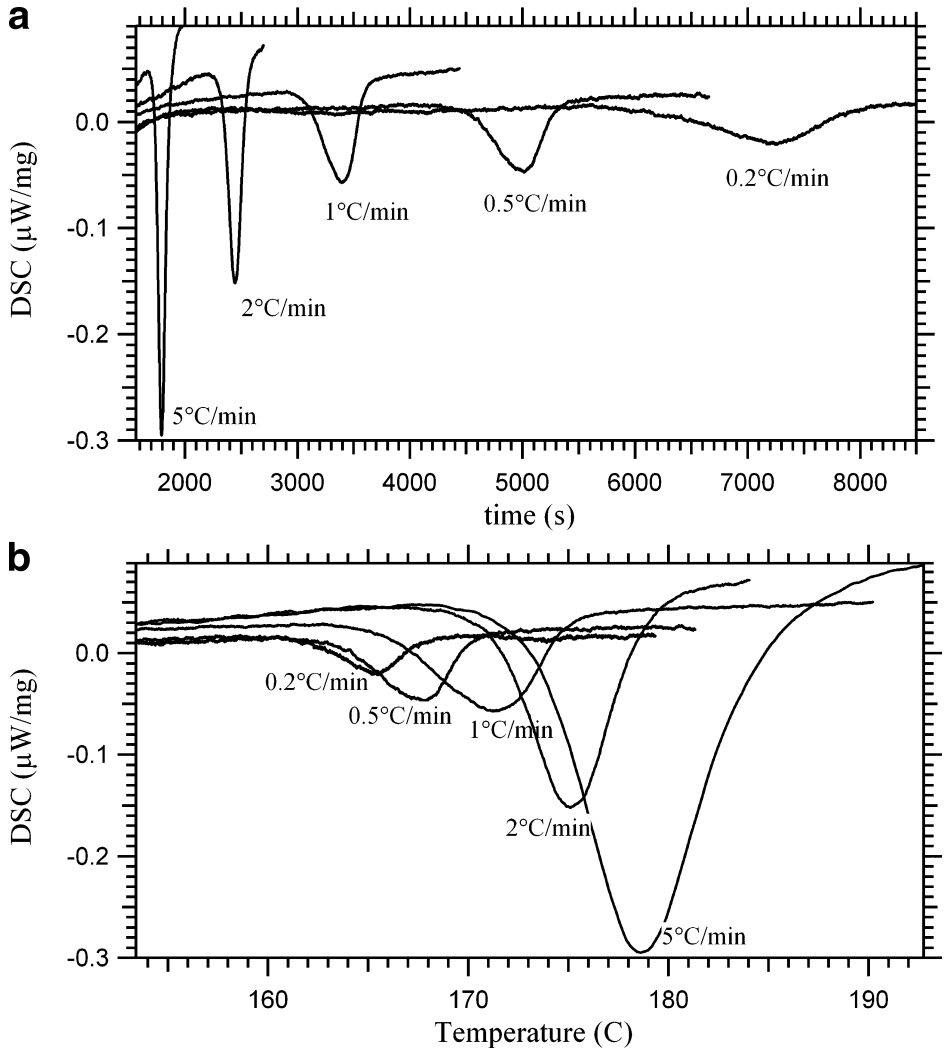

Figure 4. (a) Time dependence of the beta−delta HMX transition on the DSC ramp rate. (b) Temperature dependence of the beta−delta HMX transition on the DSC ramp rate.

therefore coherent generation of SHG, is dependent on the square of the concentration. This, in part, accounts for the very large SHG signals found for delta HMX. The mapping of the progress variable measured by SHG with delta fraction is therefore quadratic in the SHG intensity. For free space (lens coupled) SHG measurements, the dependence has been found to be between linear and quadratic. The signal is quadratic with the number of delta molecules within a crystal but linear between crystals due to the incoherence between different crystals.[12] In such measurements we assume a fully quadratic dependence, as has been discussed previously.[2] Coherent generation is only possible, however, upon coherent excitation, and for SHG measured through a fiber optic, the scrambling of phase due to multiple reflections in the fiber optic makes the SHG a linear observable with delta fraction. The concentration is therefore treated as linear in the simultaneous DSC/SHG experiments described below.

Figure 4 shows the rate dependence for the calorimetric observable of the phase transition. The beta−delta transition is endothermic and requires ~9.9 kJ/mol to complete.[7,13] Figure 4a shows the DSC versus time, and Figure 4b shows it versus temperature. The phase transition can be seen to occur at higher temperatures for faster rates, as predicted by the kinetic model of the transition described earlier. The faster ramp rates give sharper peaks, but the total endothermicity integrated under the curve is independent of ramp rate. The slower ramps give shallower peaks that become hard to separate from the baseline for very slow ramp rates (below a few tenths of a degree per minute). The onset of the endotherm for the slowest rate measured can be seen to begin at approximately 160.5 °C, which is just above the predicted equilibrium temperature of 159 °C.[7,13] As the ramp rate increases, the superheating of the sample above the equilibrium temperature increases before the onset of the phase transition is reached.

The Raman spectra collected for the beta and delta polymorphs are shown in Figure 5. There are several spectral features that can be used to distinguish the phases, most associated with ring modes. For instance, the region from 300−500 cm^{-1} is associated with ring torsion,[14,15] the 600−722 cm^{-1} range with combined ring, nonring deformations, and the 800−1000 cm^{-1} range with ring stretching.[16] Figure 5a shows the averaged Raman spectra measured for the beta and delta phases. The fluorescence background increases as the sample is heated to delta phase and the signal-to-noise is degraded by this background. In Figure 5b, the spectra have been processed using commercial smoothing and cubic baseline corrections. Removing the fluorescence baseline allows for easier identification of the spectral regions which show significant differences between the phases. By monitoring peak heights for peaks associated with either beta or delta phase, the progress between them can be tracked. Figure 6 shows the use of those features to follow the evolution on heating a sample from beta to delta phase. Data

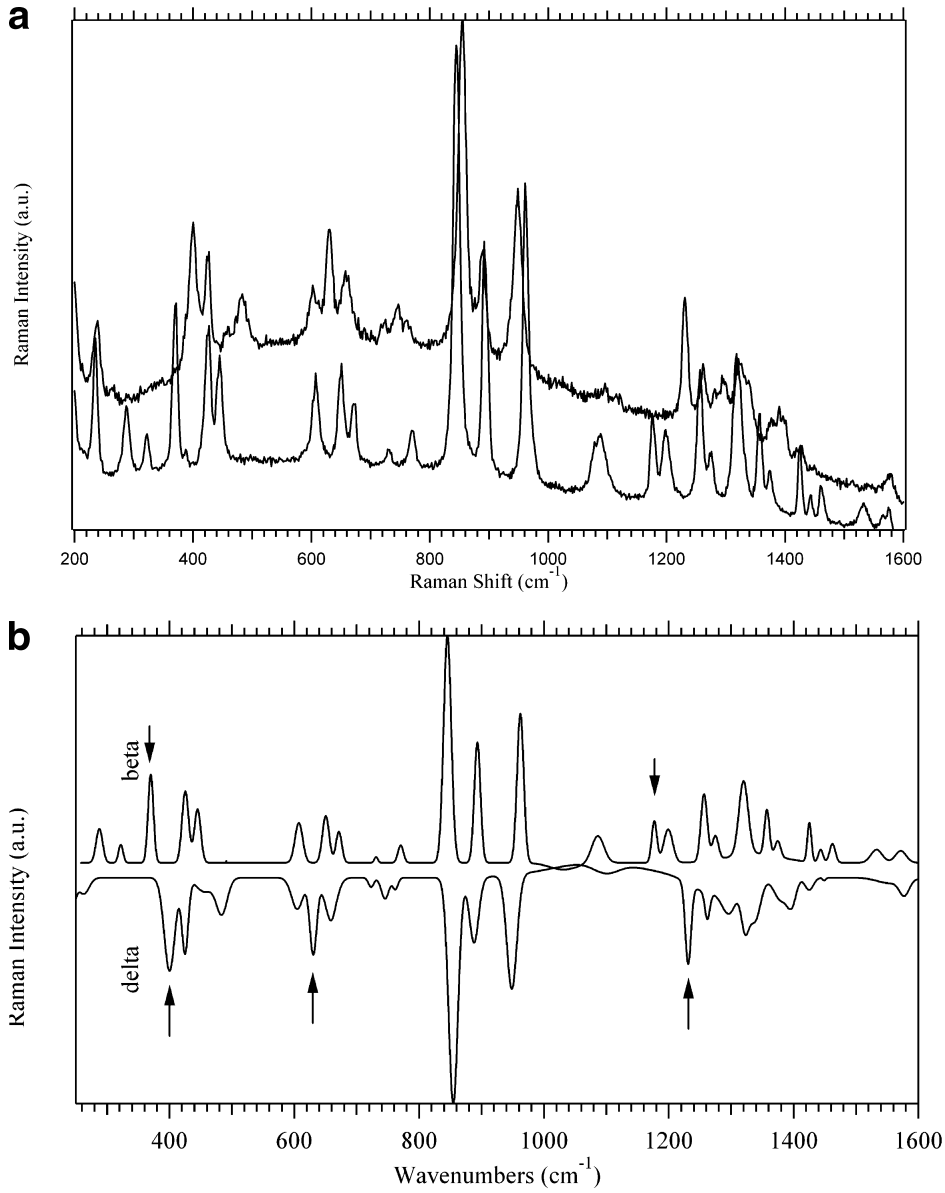

Figure 5. (a) Raman spectra of beta (thin line) and delta (thick line) PBX 9501. (b) Raman spectra of (a) subjected to baseline subtraction and smoothing. The spectral regions prominent in the analysis and peak intensity measurement are shown.

from two different experiments with different temperature/time trajectories is included on this graph. The data shown as triangles are for an experiment first heated to approximately 165 °C, then held for approximately 6200 s and then cooled back down to 125 °C to allow reversion to beta phase to occur (as evidenced by a decrease in SHG signal). The data shown as circles are for an experiment heated to approximately 164 °C and held there. The progress of the transition is measured by following peak heights specific to delta phase and by following the loss in peak height for peaks specific to beta phase. Changes in baseline and scattering efficiency with temperature are corrected out by taking the peak height relative to the off-peak signal level. Overlaid on these plots is the normalized SHG signal collected simultaneously during these experiments.

The phase transition progress measured by SHG and by DSC is directly compared for different heating rates in Figure 7a. The normalized SHG signals are shown in the solid lines for heating rate from 1 to 10 °C/min. The DSC data is collected simultaneously with the SHG in a commercial calorimeter modified to introduce a fiber optic probe above the sample pan. The fiber optic is used both for the introduction of the pump light and to collect the second harmonic light generated from the sample. Figure 7a shows the DSC endotherm and normalized SHG signals plotted versus the sample temperature at three different ramp rates. The generation of a second harmonic signal is seen to occur synchronously with the start of the endotherm. The endotherm areas cannot be directly compared when plotted against temperature rather than time as shown in Figure 4b. What can be seen in a plot verses temperature is that the highest ramp rates show phase transition onset at the highest temperature. The broadening of the curves with ramp rate is due to the larger rate rather than being a direct temperature driven kinetic effect. The DSC signal is integrated and compared to the SHG, which is an integral measure of the progress from beta to delta phase, in Figure 7b. Before integrating of the DSC endotherm peak, the baseline is subtracted.

In Figure 8, we compare the measured phase transition progress as a function of ramp rate to the predictions from the nucleation and growth model we developed for the measurements of the phase transition under isothermal conditions observed by SHG.[7] The closed circles are the positions of the endotherm peak measured in the DSC ramp experiments, the

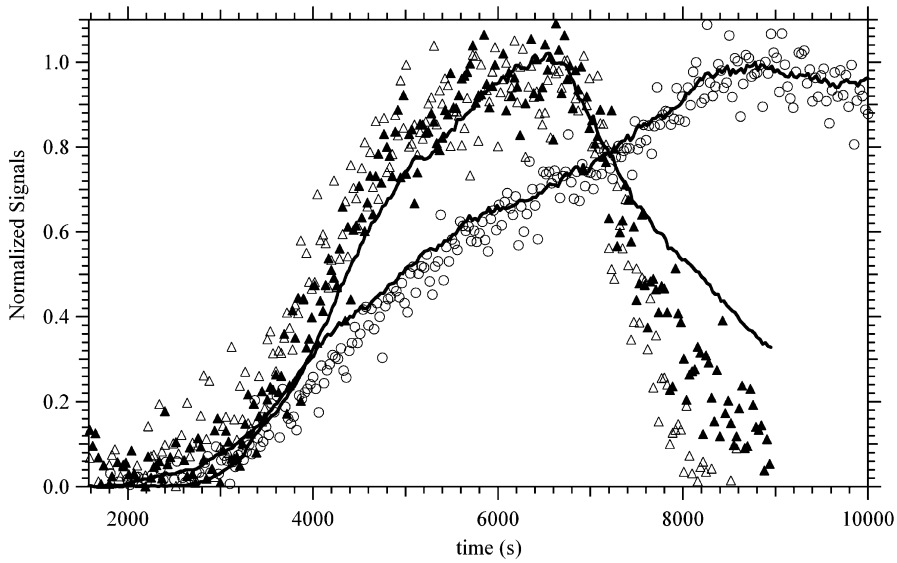

Figure 6. Normalized Raman peak intensity for delta bands (solid triangles) and SHG intensity (solid line) shown as a function of time. One minus the normalized peak intensity for beta bands (open triangles for one isothermal experiment, open circles for another) is also shown as a function of time. Data collected for two different temperature trajectory experiments is shown (triangles are for 165 °C isotherm, circles for 164 °C).

closed squares are measured by SHG, the closed triangles are measured by Raman spectroscopy, and the open triangles are data taken from the literature using X-ray diffraction as observables.[4,17] The prediction of our isothermally determined model is shown as the solid line in Figure 8.[7] Although the point of this paper is the intercomparison of experimental observables, it is pertinent to mention that distinctions between isothermal and nonisothermal behavior are often made in descriptions of the kinetic models used to describe solid state decomposition and phase transitions. However, clearly the correct mechanism should be able to capture the behavior regardless of the particular temperature trajectory followed. In fact, the use of both isothermal and nonisothermal trajectories provides more stringent tests of the proposed mechanism than either alone. The isothermal treatments are very sensitive tests of the detailed kinetics, while the nonisothermal tests can efficiently test the mechanism against a wide range of temperatures. Figure 8 shows agreement not only between data obtained by the different techniques but also between the predictions of the isothermally generated kinetic model with the data collected under nonisothermal ramping conditions. The solid line shows the model calculations for the condition at which the conversion is 50% complete. We have published several proposed models of nucleation for this transition, and the calculations of Figure 8 use the reversible first order model that we originally presented.[7] At the slowest ramp rates, we begin to see changes in the PBX 9501 that we believe are due to nitroplasticizer decomposition occurring at these temperatures on time scales that are competitive with the phase transition. The nitroplasticizer is indicated as contributing to the nucleation of the phase transition, so changes in the composition of the PBX 9501 can effect the transition kinetics.[6]

Discussion

In comparing the data from each observable, the phase transition progress is found to be in agreement, with the caveat that each of the techniques must probe a large enough volume to be representative of the heterogeneous sample. Despite providing redundant measures of phase transition kinetics, each of the techniques has different strengths and weaknesses. DSC provides an absolute differential measure of the progress of the phase transition. Integrating the area of the endotherm to generate a measured transition enthalpy and comparing that to the known enthalpy for the beta−delta phase transformation allows one to confirm the completion of the phase change. If the phase change does not go to completion, the fraction converted can be determined. This is particularly important for HMX samples where the variability in nucleation sites from crystal to crystal causes the individual crystals within a sample to transition over a broader time scale than would be predicted by the growth dominated kinetics alone.[6] The uncertainty in the DSC measurement is due to any baseline drift present. This is minimized using matching sample and reference pans and correcting out instrument drift, but still limits the technique to heating rates above a few tenths of a degree per minute.

SHG provides a relative rather than an absolute measure of phase transition progress. Due to changes in optical properties and the fact that the SHG from HMX particle beds falls somewhere between incoherent and fully coherent, turning the SHG signal into an absolute measure would be difficult. However, SHG is an extremely sensitive probe of the transition progress due to the zero background SHG for beta phase and the high SHG efficiency for delta phase. Unlike DSC, SHG measures the total fraction of delta rather than the energy of conversion from beta to delta. It is thus an integral measure and can be used to measure progress independent of the rate of conversion.

The integrated endotherm and SHG signals are seen to be in close agreement as kinetic probes. There are some artifacts which skew this agreement. The pump light for the SHG imparts a small amount of energy to the sample. Thus the SHG is probing the top surface of the sample, which is at a slightly higher temperature due to the pump and therefore begins before the bulk of the sample. This artifact is minimized by using as low a pump energy as possible and thin samples in order to maintain a more uniform temperature in the sample. However, the comparison of integrated endotherm and SHG still shows a trend of SHG onset slightly before the integrated endotherm. Additionally, the SHG is an instantaneous measure. Its response time is chosen by the integration time used for reasonable signal-to-noise ratio. For these experiments, we use a 2 s integration time. The DSC response time is a function of the thermal

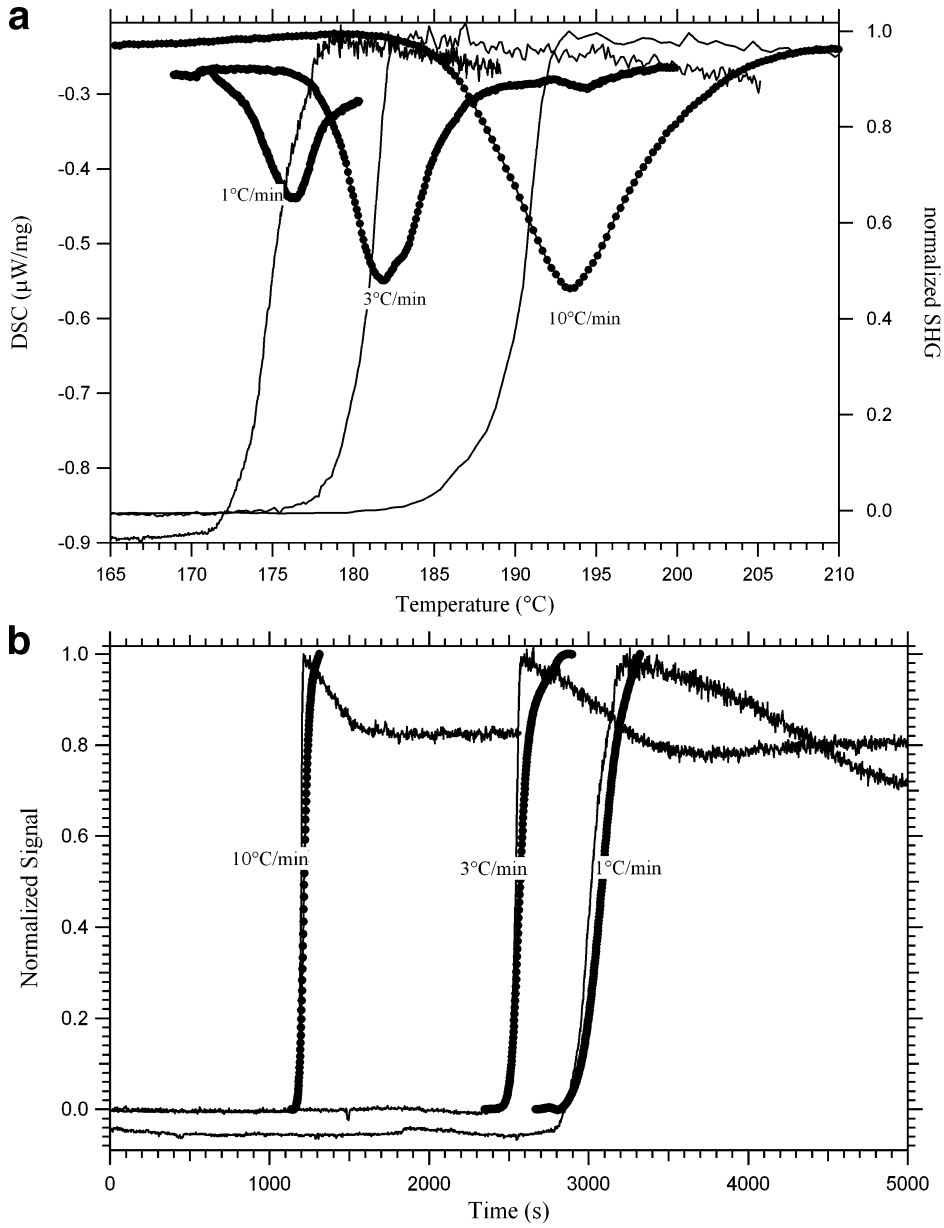

Figure 7. (a) SHG and DSC data sets measured simultaneously. Solid lines are SHG data sets at rates of 1 to 10 °C/min as indicated on the graph. Solid circles are the endotherm in μV/mg measured by DSC for each heating rate. (b) Comparison of normalized SHG (solid line) and integrated DSC (filled circles) for heating rates from 1 to 10 °C /min.

conductivity of the sample and sample pan, which we observe to be on the order of tens of seconds, adding to the lag between the onset of SHG and the endotherm.

Raman spectroscopy is also an integral measure of the delta phase. In addition, it provides more information than either DSC or SHG. SHG can sense the growth of a noncentrosymmetric phase. However, it cannot discern the presence of multiple noncentrosymmetric phases. Raman spectroscopy can be used to distinguish not only centrosymmetric from noncentrosymmetric phases, but between multiple like-symmetry phases. It can potentially be used as an absolute measure of progress between phases but is highly sensitive to background fluorescence levels, which become a large component of the signal on heating HMX due to the presence of decomposition products of HMX and binder. Raman is less sensitive than SHG since it is not a zero baseline signal. Its sensitivity is limited by the broad-band scattering and fluorescence levels. In practice, Raman can be used to sense the presence of delta phase at the percent level compared to SHG which has a low enough background to be sensitive to better than 10^{-4}.

While the data shown in the Results section above show agreement between all three observables studied, this agreement relies on the probing of sample volumes large enough to be representative of the sample. The heterogeneity of PBX 9501 implies that a statistical sampling must be made.[18,19] For an integral SHG signal, this is done by using a beam spot size large enough to sample a volume large compared to the spatial heterogeneity of the sample. For these experiments, the pump beam spot size is several millimeters in diameter. The samples consist of HMX crystals with a bimodal size distribution. The peak in the distribution for the larger crystals is over 100 μm, with a tail extending to nearly 500 μm.[18,19] For this reason, the probe region used was several millimeters. For Raman comparison, the Raman pump beam was expanded to cover the same area as the SHG probe, leading to degradation in the signal-to-noise of the collected spectrum. Higher quality spectra are

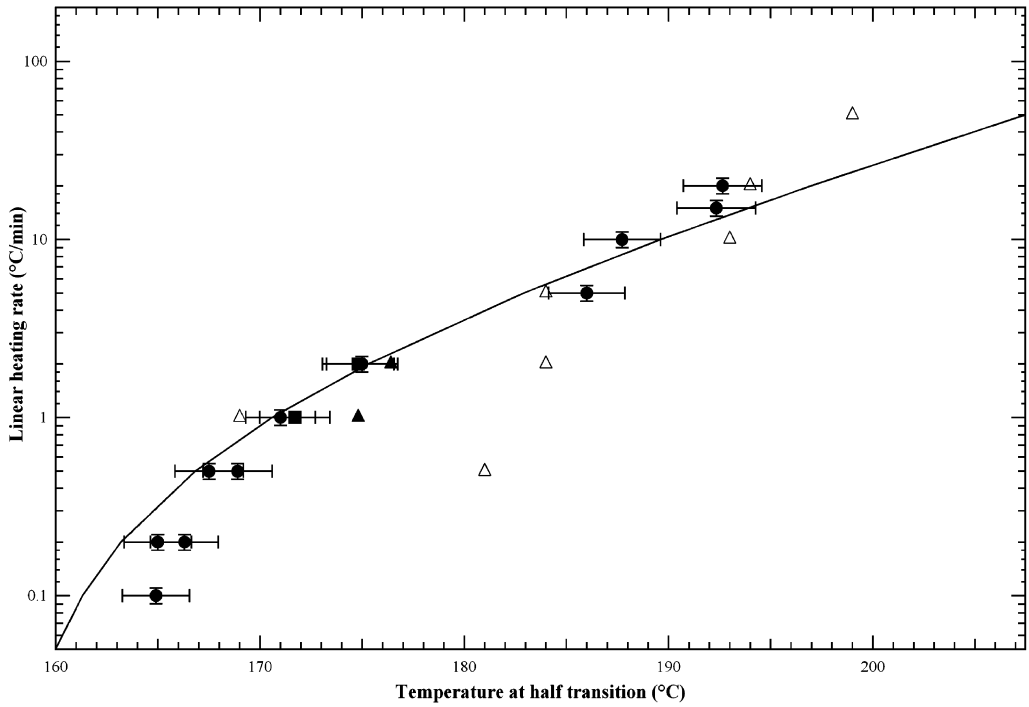

Figure 8. Comparison of phase change observables with nucleation and growth model calculations. The closed circles are the positions of the endotherm peak measured in the DSC ramp experiments, the closed squares are measured by SHG, the closed triangles are measured by Raman spectroscopy, and the open triangles are data taken from the literature using X-ray diffraction as observables.[17]

collected with a focused beam, but then multiple point collection would be necessary to build up the statistical sampling. The same would be true for any probe sampling a volume small compared to the heterogeneity of the sample. The comparison holds true for the component HMX crystals as well as for the PBX 9501 formulation. A sample size smaller than the heterogeneity of the sample would look at the growth front propagating across the region in this range of growth limited kinetics with a small number of nucleation sites. This would lead to a late measured onset, as has been previously reported in the literature and reproduced using a small beam size, either with Raman or with SHG. Integral measurements using any of the above probes—Raman, SHG, calorimetry, or volume change[5]—are all consistent.

Conclusions

We have used calorimetry to confirm the validity of SHG as a probe for the solid−solid phase transition in PBX 9501. We have also compared Raman spectroscopy as a probe of the solid−solid phase transition and found that by sampling over a volume large compared to the length scale of heterogeneity of the sample, Raman was also useful as a kinetic probe. For a symmetry changing solid phase transition, SHG provided the highest sensitivity probe because it is a zero background integral measure of the fraction of sample converted to the final phase. However, it is a relative and not an absolution measure, unlike calorimetry which can be integrated to give the total fraction of the enthalpy of the phase transition. SHG is very sensitive, for HMX especially due to phase matchability, but hard to use as an absolute measure due to light scattering properties and changes in light scattering and absorption. Raman could also be used as a progress variable. It is an integral measure, less sensitive than SHG, but can be used as an absolute progress variable. Caution must be taken for all of these probes to sample over a representative volume. For Raman, expanding the beam to sample a larger volume has the limitation that the signal quality is degraded. The signal-to-noise is also degraded by the onset of a strong fluorescence background and change in scattering efficiency in the heated samples. However, it is generally applicable and provides an integral progress variable where SHG is only useful for symmetry changing solid phase transitions.

Acknowledgment. The authors wish to acknowledge the support of the Science Campaign 2 and the Surety Program administered by Los Alamos National Laboratory, as well as the Joint Munitions Program administered by both the Departments of Energy and Defense. The authors also wish to acknowledge Dr. Jack B. Henderson of NETZSCH Instruments, Inc. for assistance with modifying the STA409 to allow for fiber optic access.

References and Notes

(1) Henson, B. F.; Asay, B. W.; Sander, R. K.; Son, S. F.; Robinson, J. M.; Dickson, P. M. *Phys. Rev. Lett.* **1999**, *82*, 1213.

(2) Smilowitz, L.; Henson, B. F.; Asay, B. W.; Dickson, P. M. *J. Chem. Phys.* **2002**, *117*, 3789.

(3) Saw, C. K.; Zaug, J. M.; Farber, D. L.; Weeks, B. L.; Aracne, C. M. *AIP Conf. Proc.* **2002**, 856.

(4) Weeks, B. L.; Ruddle, C. M.; Zaug, J. M.; Cook, D. J. *Ultramicroscopy* **2002**, *93*, 19.

(5) Gieske, J. H.; Miller, J. C.; Renlund, A. M.; Tappan, A. S. Raman Spectroscopic and Ultrasonic Measurements to Monitor the HMX Phase Transition, 1999.

(6) Smilowitz, L.; Henson, B. F.; Greenfield, M.; Sas, A.; Asay, B. W.; Dickson, P. M. *J. Chem. Phys.* **2004**, *121*, 5550.

(7) Henson, B. F.; Smilowitz, L.; Asay, B. W.; Dickson, P. M. *J. Chem. Phys.* **2002**, *117*, 3780.

(8) Levitas, V. I.; Smilowitz, L. B.; Henson, B. F.; Asay, B. W. *Appl. Phys. Lett.* **2006**, *89*.

(9) Bourhill, G.; Mansour, K.; Perry, K. J.; Khundkar, L.; Sleva, E. T.; Kern, R.; Perry, J. W.; Williams, I. D.; Kurtz, S. K. *Proc. SPIE—Int. Soc. Opt. Eng.* **1993**, *1853*, 110.

(10) Kurtz, S. K.; Perry, T. T. *IEEE J. Quantum Electron.* **1968**, 333.

(11) Shen, Y. R. *The Principles of Nonlinear Optics*; John Wiley: New York, 1984.
(12) Andrews, D. L.; Allcock, P.; Demidov, A. A. *Chem. Phys.* **1995**, *190*, 1.
(13) Cady, H. H.; Larson, A. C.; Kromer, D. T. *Acta Crystallogr., Sect. B* **1963**, *16*, 617.
(14) Goetz, F.; Brill, T. B.; Ferraro, J. R. *J. Phys. Chem.* **1978**, *82*, 1912.
(15) Goetz, F.; Brill, T. B. *J. Phys. Chem.* **1979**, *83*, 340.
(16) Iqbal, Z.; Bulusu, S.; Autera, J. R. *J. Chem. Phys.* **1974**, *60*, 221.
(17) Herrmann, M.; Engel, W.; Eisenreich, N. *Z. Kristallogr.* **1993**, *204*, 121 Part 1.
(18) Liu, C. *Exp. Mech.* **2005**, *45*, 238.
(19) Clements, B. E.; Mas, E. M. *Modell. Simul. Mater. Sci. Eng.* **2004**, *12*, 407.

JP902111C